GEMINI

The Innermost Secrets of CCDs

Prompted by recent discussions about sampling effects within CCD pixels (see article on page 7) we have made detailed measurements of the sensitivity across the surface of a CCD. The CCD is well known as a two-dimensional array, with periodic structure which establishes individual picture elements (pixels). Less widely known is the fact that the CCD array has a significant internal structure, on a sub-pixel spatial scale, which gives rise to periodic variations in response along both axes of the device. This modulation of response is particularly relevant when the data is spatially undersampled, and could affect many areas of use including photometry, spectroscopy, and astrometry.

The internal structure of a CCD

Figure 1 illustrates the internal architecture of a CCD, and emphasises the

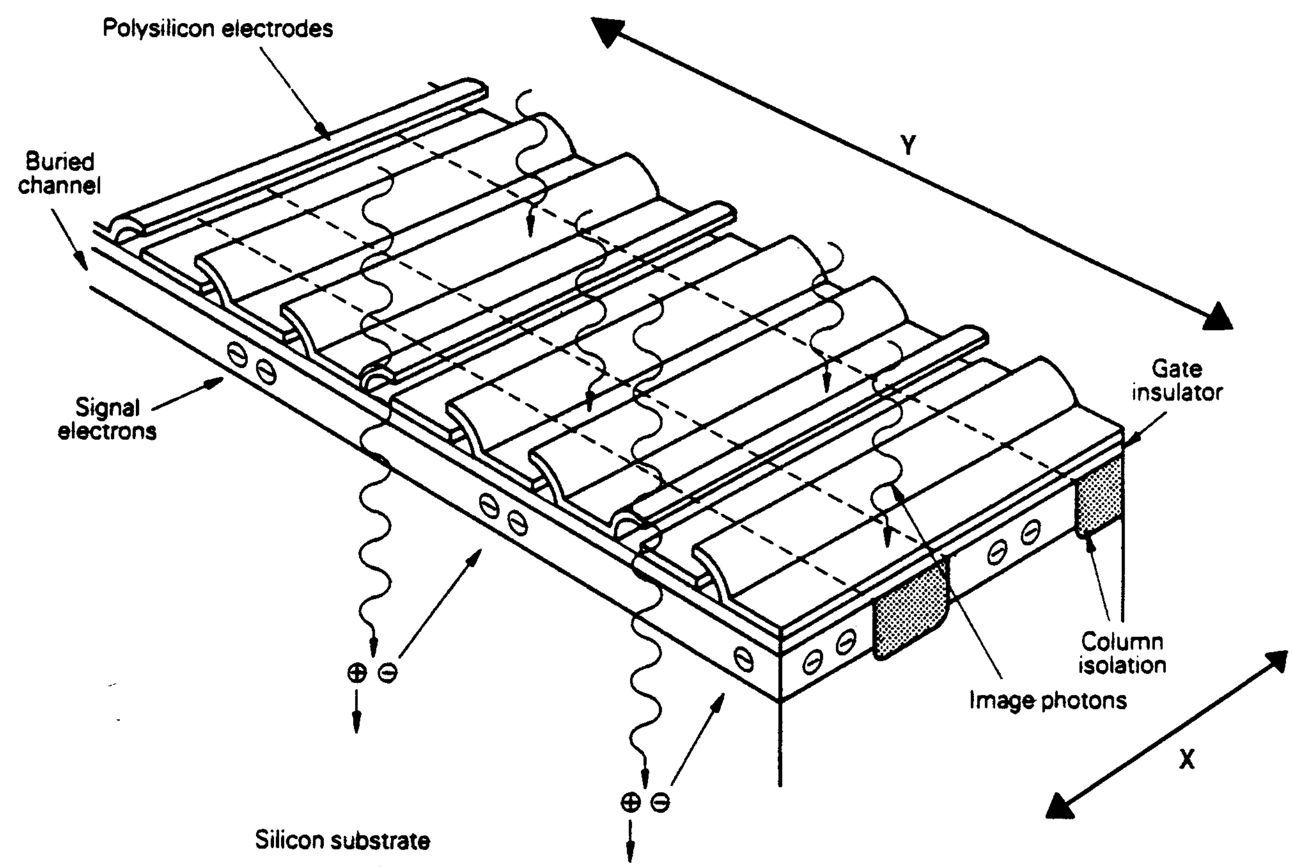

Fig 1 – Section of a CCD image sensor.

Issue 41, Sept 93

considerable amount of inner structure. It may be seen that in the *Y* (column) direction the electrodes have a periodic structure on the surface of the CCD. However, in the *X* (row) direction there is an internal (channel stop) barrier as well as some surface structure (not shown in our figure).

The physical orientation of the CCD with respect to the telescope/instrument focus is arbitrary. On the INT and WHT Faint Object Spectrographs (FOS) we have chosen to use *X* for the spatial direction and the (longer) *Y* dimension for dispersion. In contrast, on the IDS and ISIS we have chosen *X* to be the dispersion direction for both the EEV and Tektronix CCDs used on these instruments.

We do not intend in this paper to discuss the intimate details of the CCD construction, but rather to quantify the effects of sub-pixel structure. We are in the process of understanding all the mechanisms that can introduce a spatial modulation of response; some of them are merely listed below.

- Thickness variations in the surface structures introduce changes in the optical absorption (light losses); these will be weak functions of wavelength.
- Thickness variations of the surface introduce optical interference which may enhance or reduce the optical response.
- Changes in internal structure (eg the channel stop) can cause a variation in efficiency of signal collection.

Additionally, our CCD has a dye coating which is not illustrated in the figure. This coating should absorb UV/blue photons fairly uniformly and then re-emit green/red ones for subsequent absorption by the CCD. This means that short-wavelength spatial response modulation should look similar to the green/red modulation.

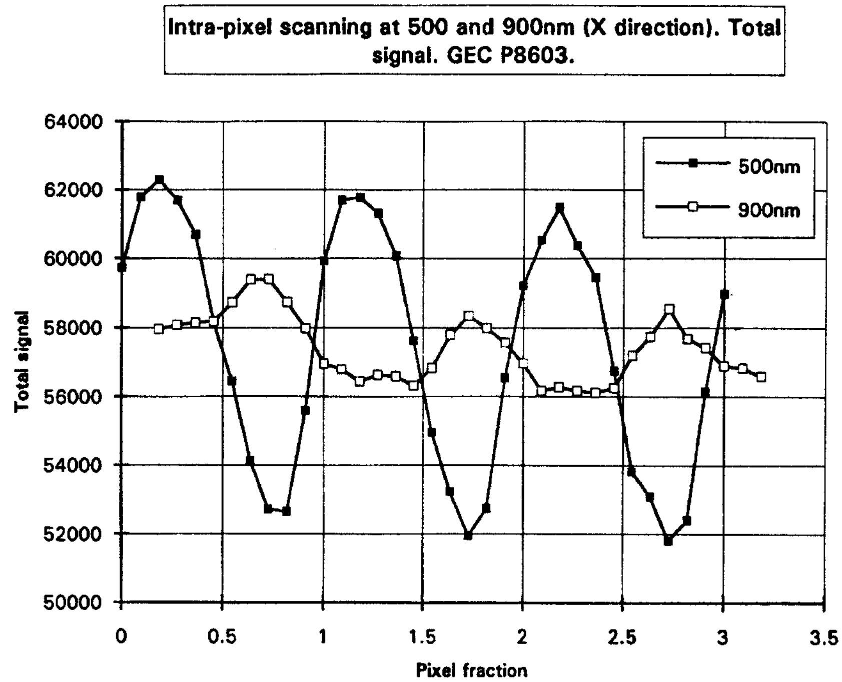

Fig 2 – Total measured signal as a function of pixel position in the X (serial) direction. Plots are shown for 500 and 900 nm spatial scans.

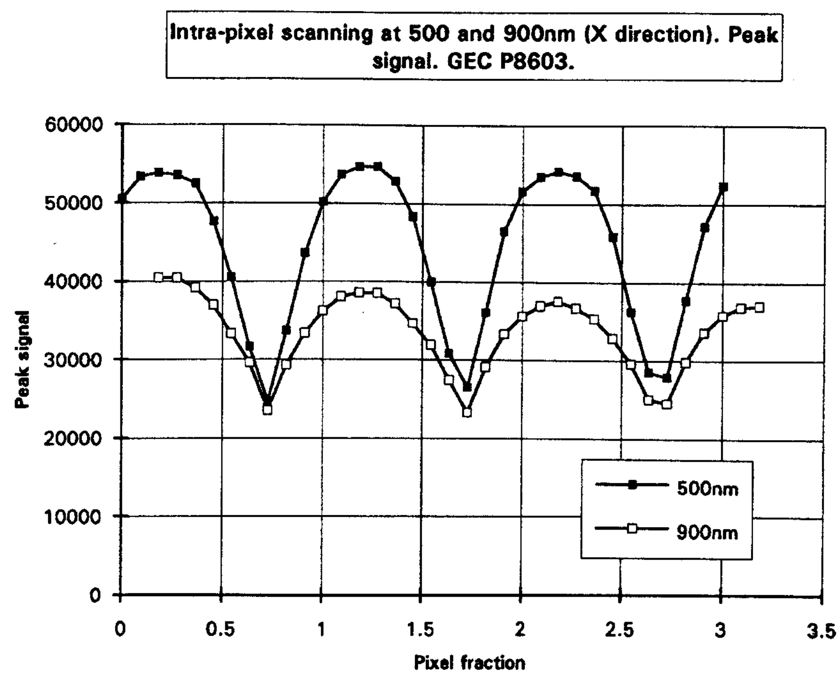

Fig 3 – Peak signal as a function of pixel position in the X (serial) direction. Plots are shown for 500 and 900 nm spatial scans.

In order to investigate the internal sensitivity structure of a CCD we arranged to project a small spot of light

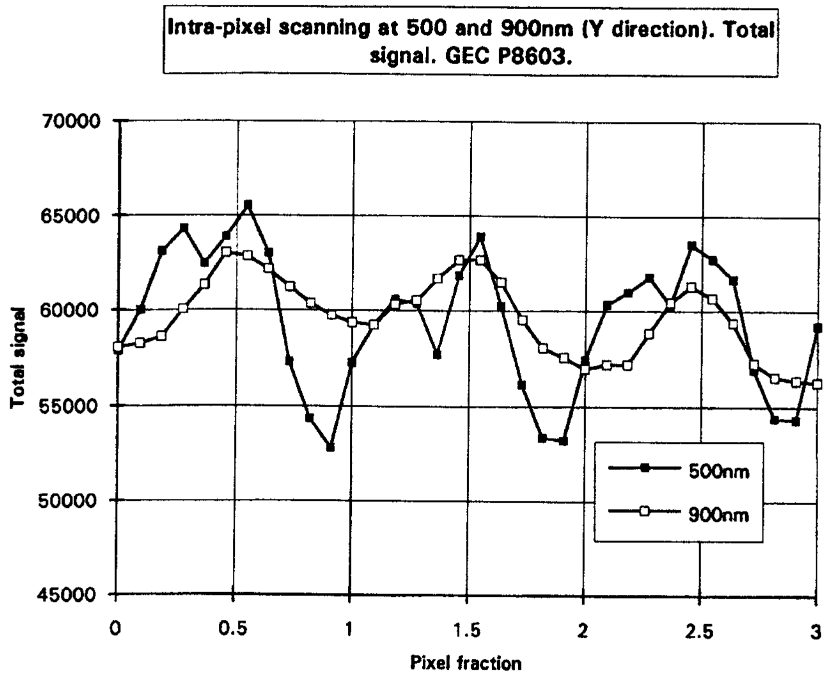

Fig 4 – Total measured signal as a function of pixel position in the Y (parallel) direction. Plots are shown for 500 and 900 nm spatial scans.

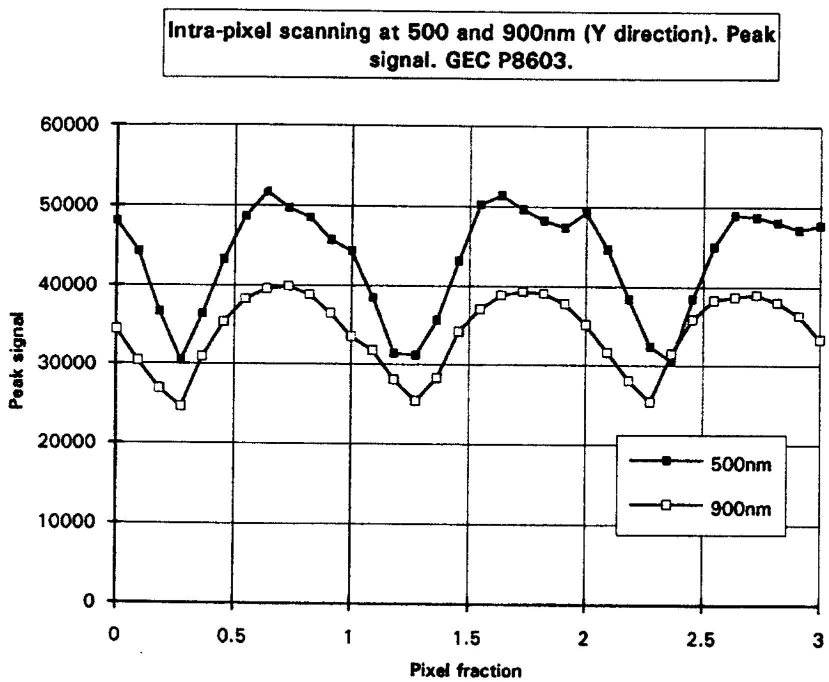

Fig 5 – Peak signal as a function of pixel position in the Y (parallel) direction. Plots are shown for 500 and 900 nm spatial scans.

on to the CCD. The spot was mechanically moved across the surface, and images were recorded at each position.

The experimental arrangement

A 25 μm pinhole was projected, via a 10:1 demagnifying lens, on to the surface of a CCD. A colour filter was used to define the wavelength. The lens had the additional benefit of demagnifying the movement of the pinhole; hence standard *X/Y* micrometer slides permitted movement in steps of 2 μm projected on to the CCD.

In this context we shall refer to *X* as the horizontal (row) direction on the CCD, *Y* as the vertical (column) direction, and *Z* as the axial (focus) direction.

After setting up the pinhole and lens system, we used a microscope objective to measure the actual projected diameter of the spot.

We made measurements on a standard cryogenically cooled GEC/EEV P8603 CCD, with an ESO dye-coating. Our test CCD was essentially the same as that installed in the ING FOS instruments. This device has pixels of size 22.0 μm square, and was operated at a temperature of 150K.

The measurements in detail

The spot was focussed carefully (at each wavelength used), and its exact size measured. At 500, 600 and 700 nm the spot had a size close to 2.5 μm; at 900 nm the spot size was below 3.5 μm; at 400 nm the spot size was about 4.5 μm. The filters had a bandpass of 10 nm.

Prior to each sequence of measurements the projected spot position was adjusted for its initial position in *X* and *Y*. The initial position was chosen in order to give a maximum signal; in fact this was not always the exact case, but nevertheless all scans had a well-defined (repeatable) starting point. An incremental scan in the *Y* direction was performed – the spot was moved in 2 μm steps over a span of 66 μm (3 pixels). The spot was then returned to its original position, and a similar incremental *X* scan was performed over 3 pixels.

For some wavelengths the process was repeated in order to estimate the noise level and precision of the scan. The duplicate scan was found to be almost identical to the first, and after subtracting the two we derived an rms standard deviation of less than 2% of the mean, indicating an excellent repeatability and good signal-to-noise ratio. In the plots presented in this article the size of the plot-symbols approximates to the magnitude of this formal error.

At selected wavelengths (500, 700 and 900 nm) we measured a complete 2-D matrix of samples over a pixel. The spot position was moved in a 3 μm grid of points (8 × 8 samples) to cover the whole pixel. At each position an exposure was taken, and the image subsequently analysed.

The camera lens selected for the first set of measurements (500-900 nm) was found to have very poor blue wavelength transmission. We were forced to use a lower quality lens for the 400 nm measurements.

For each image, the signal intensity was measured within a 3 × 3 group of pixels; less than 2% of the signal was found outside this central area. With the spot centred, most of the signal falls in one pixel, with a few percent in the adjoining ones. When the spot falls on a pixel boundary the signal is divided between two pixels, and their neighbours show a very small additional signal.

The peak signal is recorded, as well as the total (integrated) signal for the group. The projected spot may lie entirely within one pixel or be divided equally between four; hence the peak signal varies appreciably (up to 4:1) with sub-pixel position. The total signal shows some modulation, which should be interpreted as a change in overall response as a function of where the incident light falls.

The results

We shall not present the complete data set here; instead we show representative results and a summary of them all.

Figures 2 and 3 show the results of scanning in the *X* direction at wavelengths of 500 and 900 nm; the modulation of total signal and peak signal are shown respectively. Note that pixel position ~0.7 indicates the loca-

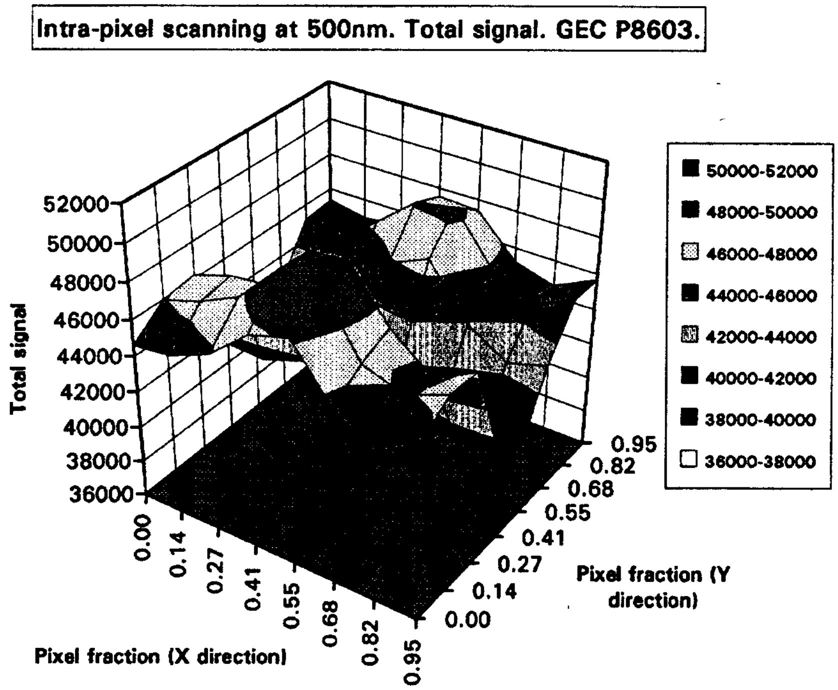

Fig 6 – Two-dimensional profile of spatial modulation, total measured signal, at 500 nm.

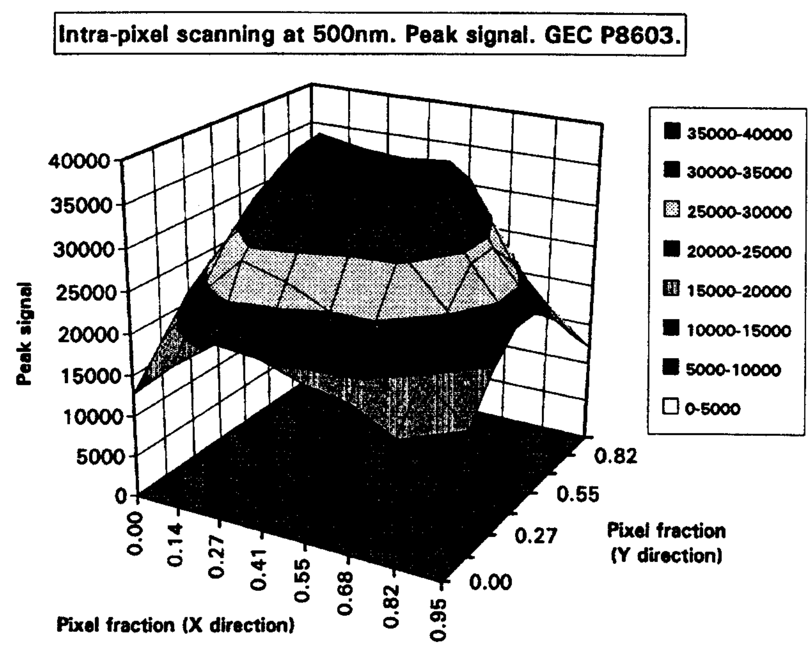

Fig 7 – Two-dimensional profile of spatial modulation, peak signal, at 500 nm.

tion of the channel stop or pixel boundary quite clearly. Similarly, figures 4 and 5 show the same types of data for the *Y* direction scans.

In all the plots, the signal level is indicated in digital units (ADU); the scaling factor is the same at any one wavelength on each plot.

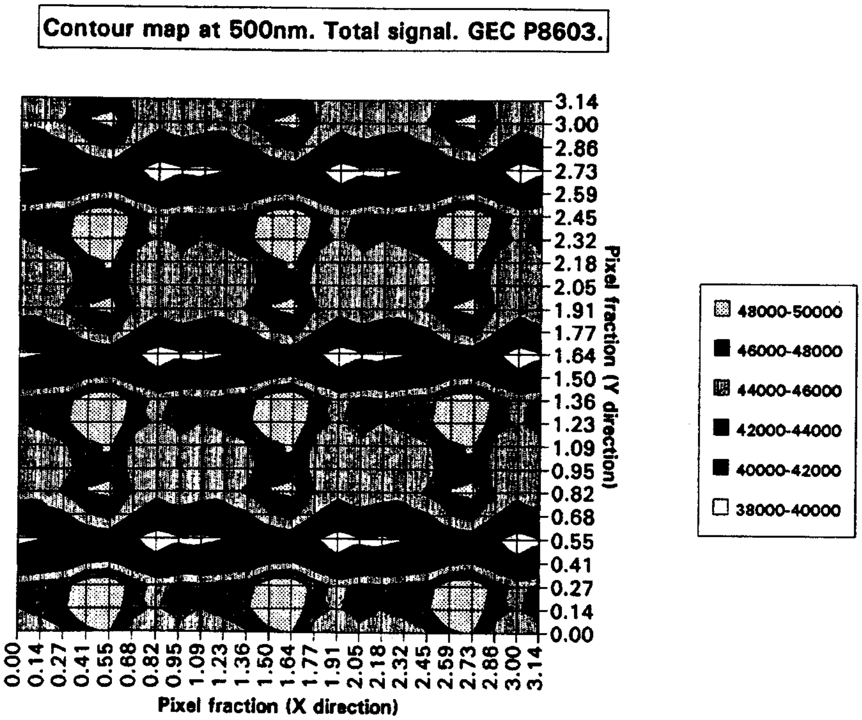

Fig 8 – Contour map representation of two-dimensional intra-pixel response; total measured signal at 500 nm.

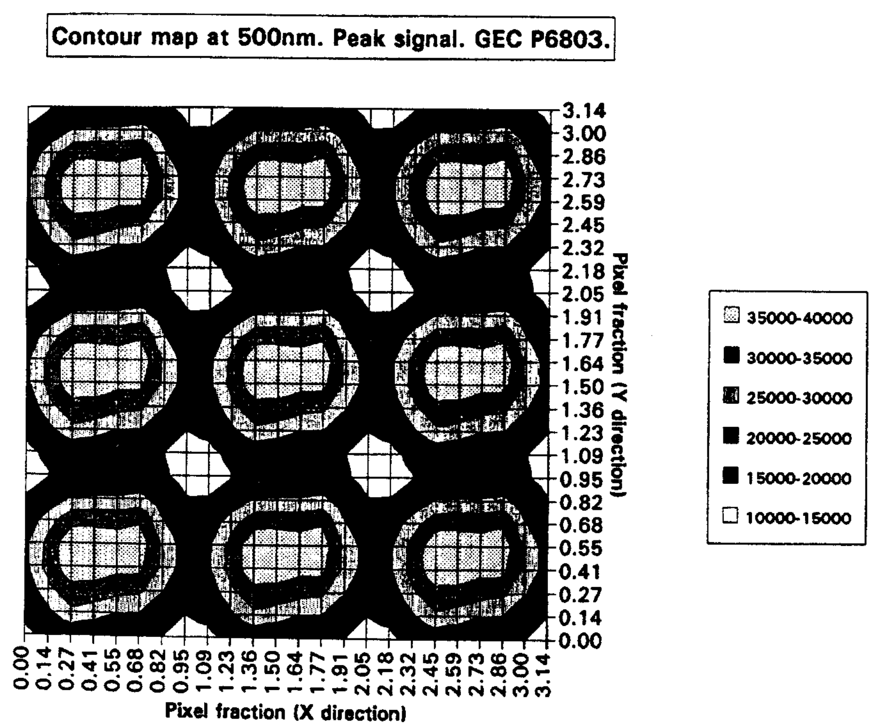

Fig 9 – Contour map representation of two-dimensional intra-pixel response; peak signal at 500 nm.

In *X*, the peak signal curves show spatial features, as well as the effects of charge-sharing when the projected spot falls midway between two pixels (on the channel-stop). The total curves demonstrate that total measured signal does vary, depending on where the illumination falls. At the shorter wavelength, signal response is minimum at the pixel boundary; however, at the longer wavelength the signal response is greater at the pixel boundary.

In *Y*, we again see a modulation of response with spatial position. In this case, the absolute pixel boundary has less meaning since the pixels are merely defined by which electrode(s) are set to be high or low in voltage. The structure is also more complex because of the triple electrode structure within a pixel.

Many of the plots show a slight linear gradient over the three pixels scanned. We suspect that this imperfect repetition from one pixel to the next has two causes. The demagnification was 9.9 rather than 10.0, hence the scan steps were slightly more than 2 μm, so the pixel pattern does not repeat exactly. In addition, the scan axes may not have been perfectly aligned with the CCD axes, leading to a slightly diagonal movement. These effects are very minor and do not affect the nature of the structure determined within one pixel.

Some of the plots appear to be noisy (especially *Y*-profiles at 500 nm). The variations from one pixel to another actually represent genuine variations in signal with position. However, we cannot yet say whether this was due to slightly imperfect scan-axes alignment, or due to actual changes in structure from one pixel to the next.

In order to illustrate the spatial structure, figures 6 and 7 show a 3-D plot of the total signal and peak signal respectively (at 500 nm only). Figures

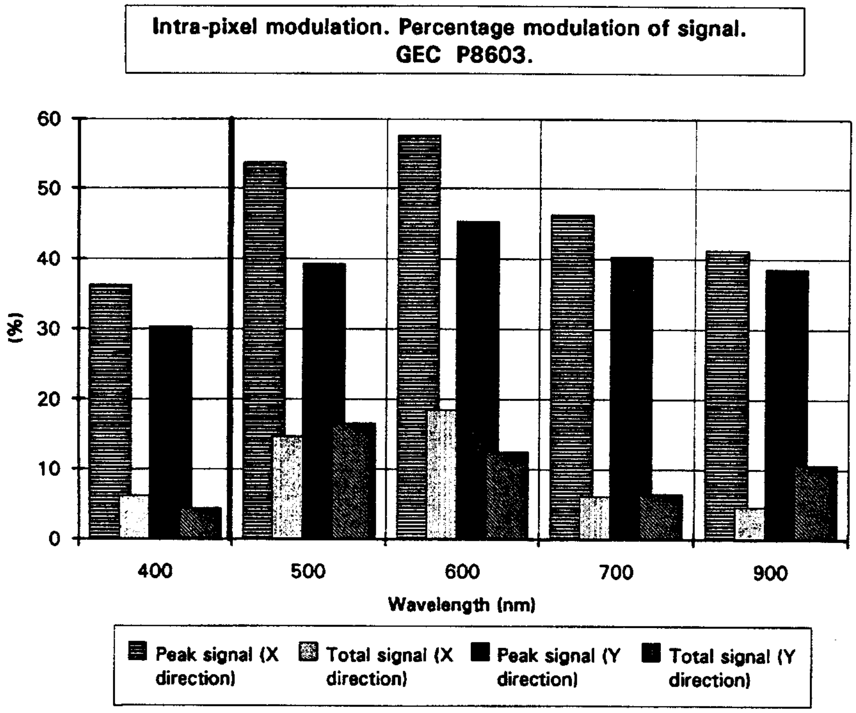

Fig 10 – Summary of spatial response results; percentage signal modulation at each wavelength.

8 and 9 show the same data, plotted as a contour map, and replicated over a 3 × 3 pixel grid.

The total signal plots show the modulation in responsivity with sub-pixel position; these are appropriate data to take when considering instrumental spatial response variations. The peak plots help to delineate pixel boundaries, but primarily show the effects of charge-sharing between pixels as a function of spot position.

As indicated above, these measurements have been made at a variety of wavelengths. Figure 10 presents a summary of the data for all wavelengths.

Some explanations

A full physical model of the optical response at all points within a CCD pixel is complex. From our initial studies of this we are confident that most of the features in our observations can be explained. It is clear that optical interference within the surface layers is an important effect. The change in optical absorption as a function of material layer and depth also contributes substantially to the response.

We have modelled the structure of the CCD, allowing for thickness variations: convolving our ~3 μm spot with this structure gives spatial-reponse curves that seem in general accord with our observations. However, at present, we have several unknown parameters which prevent a complete quantitative model.

Final comments

Of course, all of these effects become irrelevant if the CCD is used to sample the spatial structure of an object fully. For the instances where this is not possible (or desirable) we hope that our measurements will clarify the position.

Our next step will be to repeat the tests on a thinned Tektronix 1024 CCD and a coated EEV-05-30 CCD. These measurements will be made shortly and the results published; anyone interested in the results should contact the authors.

We acknowledge the assistance of Sue Worswick and Percy Terry in setting up the experiments. We thank David Burt of GEC who contributed substantially to our understanding of the internal structure of the CCD. This article was partly prompted by Vik Dhillon's discussion about FOS sampling, and we acknowledge useful discussions with him.

Paul Jorden, Jean-Marc Deltorn,
Paddy Oates, RGO